The Zeeman effect causes the spectral lines of molecular oxygen to split in the upper atmosphere under the influence of the Earth's magnetic field. This can produce measured satellite brightness temperatures that are several kelvin different relative to simulations that do not include Zeeman splitting. In order to utilize temperature sounding microwave channels that measure at levels around 30 km (12 hPa) or above, such as channels 19-22 of SSMI/S or channel 15 of ATMS, the effect must be included in the observational operator. This work presents Zeeman affected radiance simulations of such satellite channels using RTTOV, the fast radiance transfer model. Modified routines are implemented in AMSUTRAN, the line-by-line code that trains the coefficients, and RTTOV, via fast predictors that include magnetic field strength and the angle between the magnetic field and satellite viewing angle.

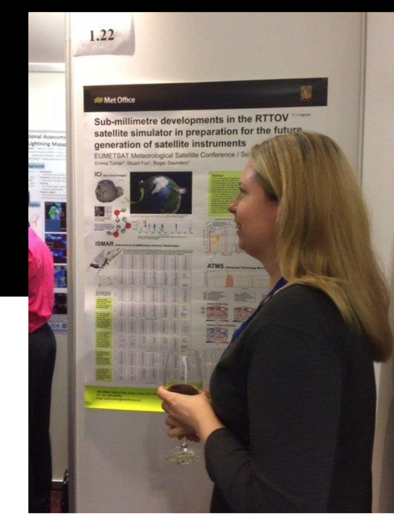

The Zeeman effect in RTTOV

Emma Turner[1], Peter Rayer[2], James Hocking
[1]emma.turner@metoffice.gov.uk, [2]retired

Zeeman transitions

Zeeman transitions in $^3O_2$ are due to the interaction of molecular spin and an external magnetic field. Splitting affects the magnetic-dipole transitions in the 60-GHz oxygen complex, which are themselves due to the interaction of spin and molecular angular momentum.

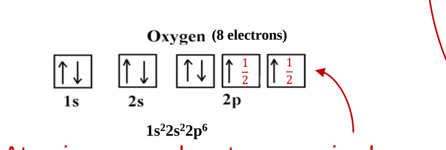

Atomic oxygen has two unpaired electrons due to Hund's rule

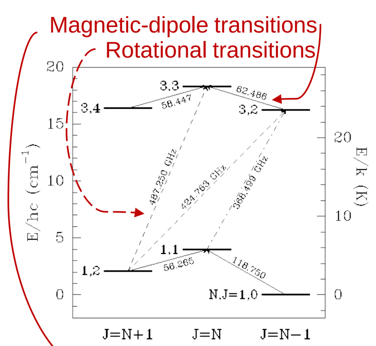

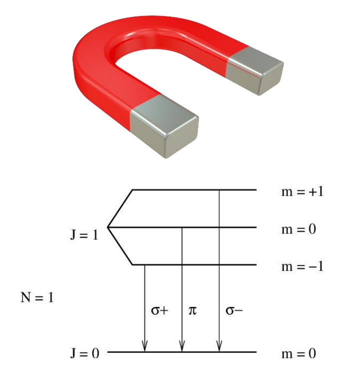

An external magnetic field splits the fine-structure lines further, of order 1-2 MHz

$(\sigma_{2s})^2(\sigma^*_{2s})^2(\sigma_{2px})^2(\pi_{2py},\pi_{2pz})^4(\pi^*_{2py},\pi^*_{2pz})^2$

$^3O_2$ also has two unpaired electrons giving a non-zero value of spin, S = 1

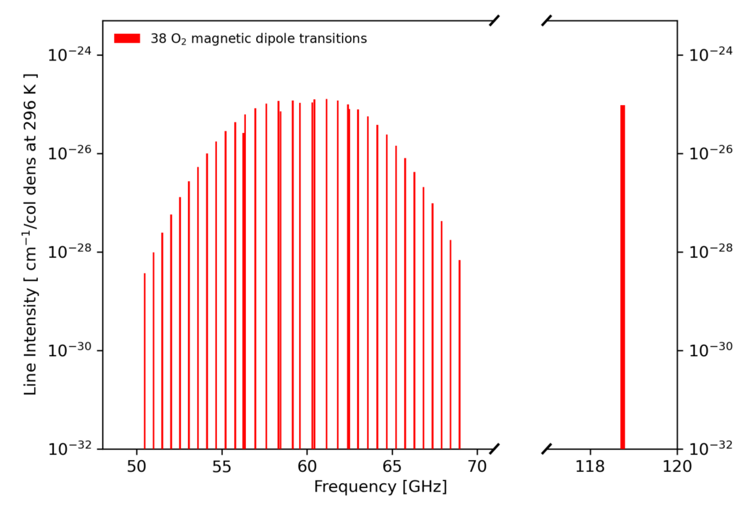

Spin-orbit coupling produces 37 fine-structure transitions between 50 and 70 GHz, and one at 118 GHz

Training data

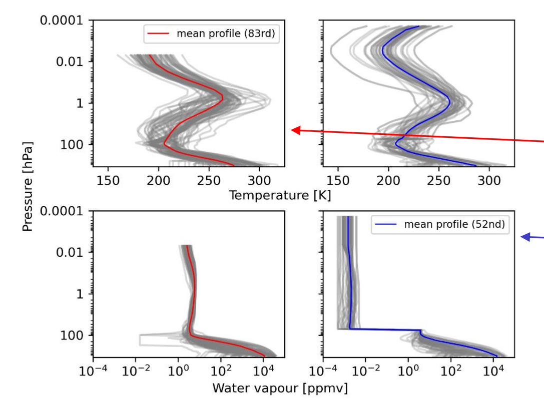

RTTOV microwave coefficients are trained on a diverse set of 83 atmospheric model profiles on 54 pressure levels, up to 0.005 hPa. Zeeman coefficients require enhanced vertical coverage at upper levels so a new set of 52 composite profiles on 84 levels, up to 0.0002 hPa, was generated.

AMSUTRAN was modified to include two extra loops over 11 values of two magnetic variables (Table 1.)

BFIELD [G]	0.2	0.25	0.3	0.35	0.4	0.45	0.5	0.55	0.6	0.65	0.7

COSBK	-1.0	-0.8	-0.6	-0.4	-0.2	0.0	0.2	0.4	0.6	0.8	1.0
BK [°]	180	143	127	114	102	90	78	66	53	36	0

Table 1. The values of total magnetic field strength **BFIELD**, in units of Gauss, and the values of cosine of the angle between BFIELD and satellite viewing angle, **COSBK**, used to generate the extended set of training Zeeman transmittances in the line-by-line code, AMSUTRAN.

	No Zeeman	Zeeman	Zeeman2
Zeeman routine	None	Rosenkranz & Staelin (1988)	Larsson et al. (2019)
Theory	First order line mixing	Hund case (b)	g-factors
Number of O_2 lines	44	34	37
Line database	Tretyakov et al. (2005)	HITRAN 1996 (apart from 118 GHz)	Tretyakov et al. (2005)
Line shape	Van-Vleck Weisskopf	Voigt	Voigt (double precision)

Table 2. O_2 absorption routines in AMSUTRAN. Zeeman and Zeeman2 are adapted from the 2019 version of the Rosenkranz (2017) code stored in a repository at http://cetemps.aquila.infn.it/mwrnet/lblmrt_ns.html. The no Zeeman routine is based on MPM92 with modified lines.

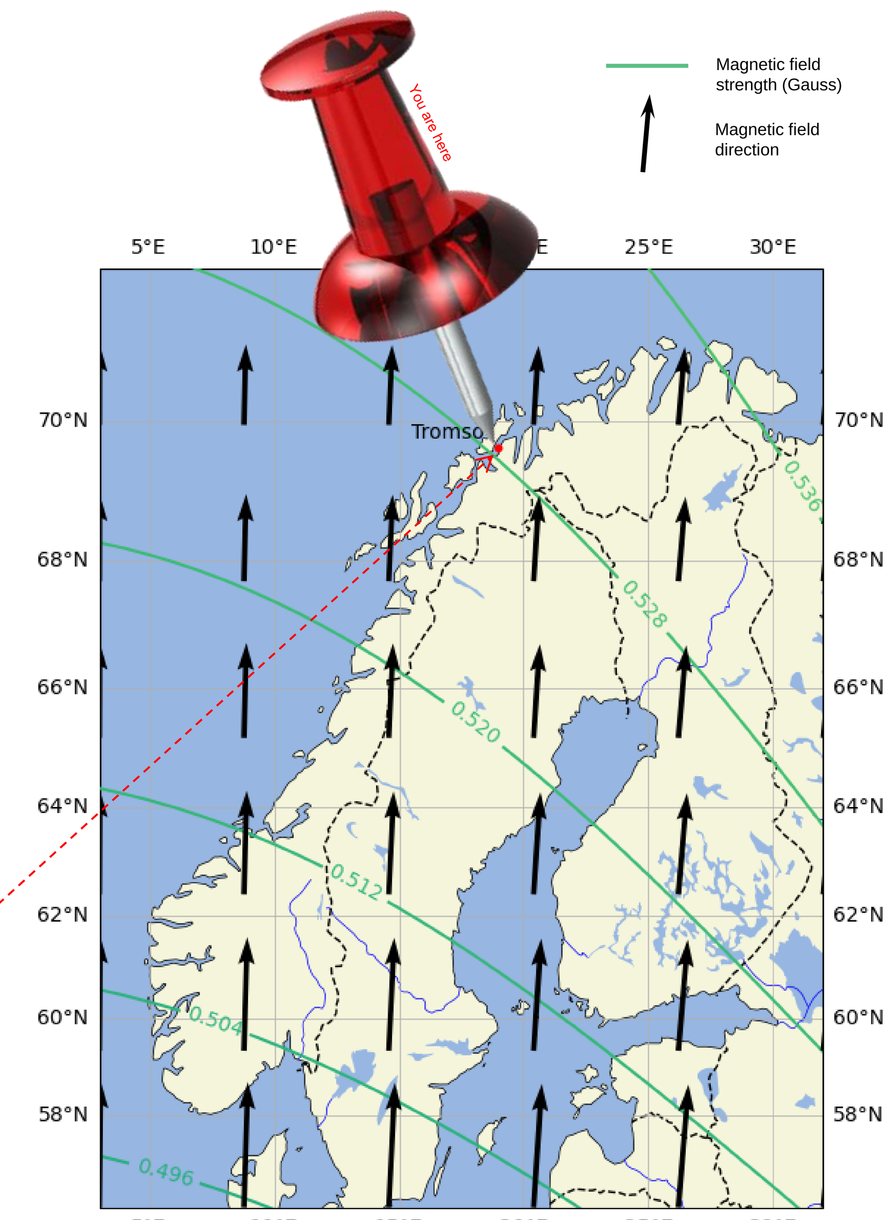

	RTTOV v13	ATMS/AMSU-A Channels 15/14	SSMI/S Channels 19-20	SSMI/S Channels 21-22
1	PATH	PATH	PATH	PATH
2	$PATH^2$	$PATH^2$	PATH * 300/T	PATH * 300/T
3	PATH * T/T_{ref}	PATH * T/T_{ref}	PATH * $COSBK^2$	PATH * $COSBK^2$
4	PATH * $(T/T_{ref})^2$	PATH * $(T/T_{ref})^2$	PATH * 300/T / BFIELD	PATH * BFIELD
5	T/T_{ref}	PATH * $COSBK^2$	PATH * 300/T *$COSBK^2$	PATH * $BFIELD^3$
6	$(T/T_{ref})^2$	PATH * $BFIELD^2$	PATH / BFIELD	PATH * $COSBK^2$ * BFIELD
7	PATH * $\sum_{lay}^{top}(dP * P * T) / \sum_{lay}^{top}(dP * P * Tref)$	PATH * $BFIELD^3$	PATH / $BFIELD^2$	PATH * $COSBK^2$ * $BFIELD^2$
8	PATH * $(T/T_{ref})^3$	$(PATH * COSBK * BFIELD)^2$	PATH * $COSBK^2$ * $BFIELD^2$	
9	PATH * √PATH * √(T/T_{ref})			
10	1			

Table 3. RTTOV predictors for mixed gases in RTTOV v13 (Hocking et al. 2021), and the equivalent Zeeman predictors for specific instruments and channels. **PATH** is the secant of the satellite viewing angle. **T** and **P** are layer temperature and pressure, respectively, and **ref** is short for the reference atmospheric profile.

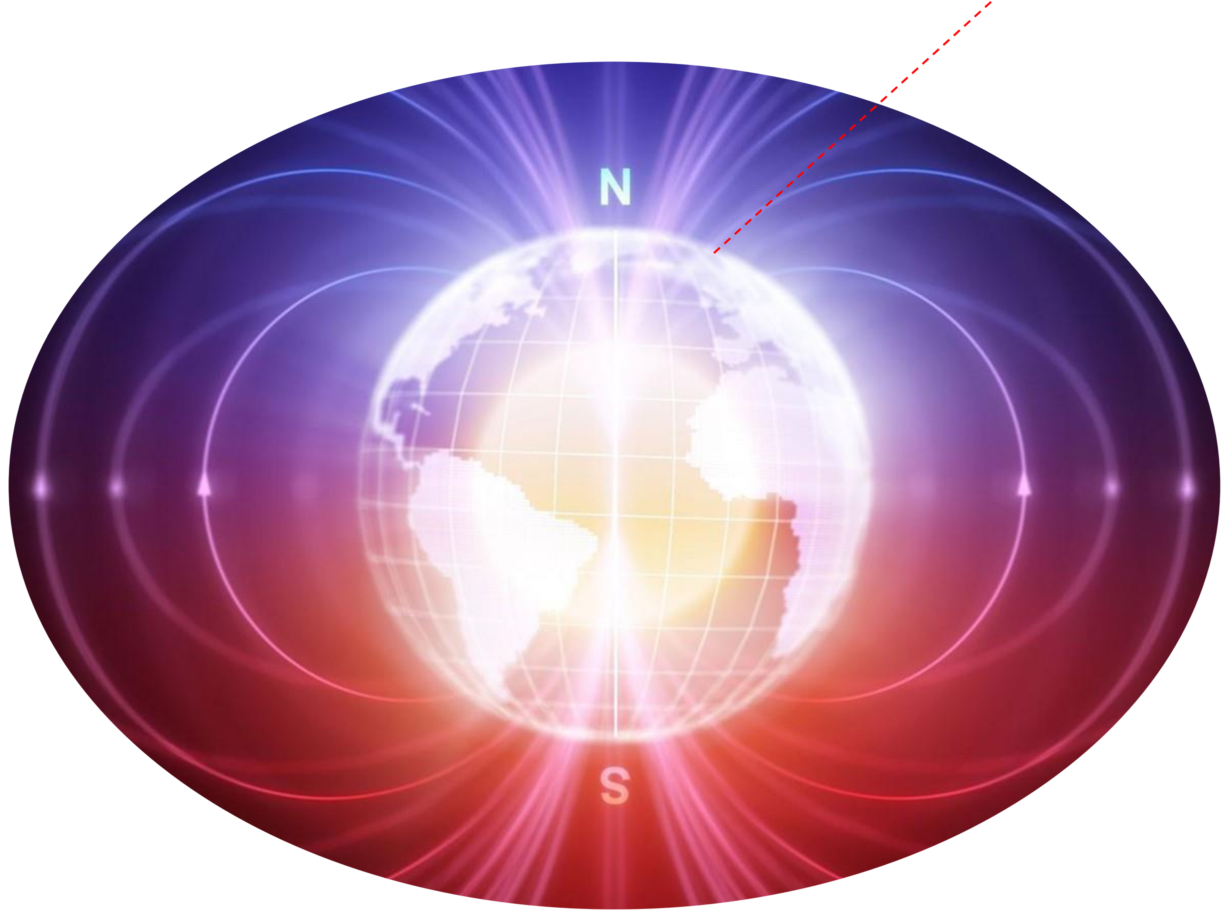

Magnetic data

Gridded x, y and z components of the Earth's magnetic field are from the International Geomagnetic Reference Field (Alken et al. 2021). One value of satellite zenith/azimuth angle is specified for each global grid of COSBK values.

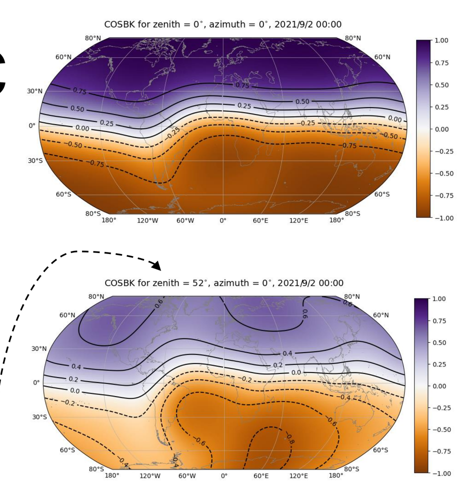

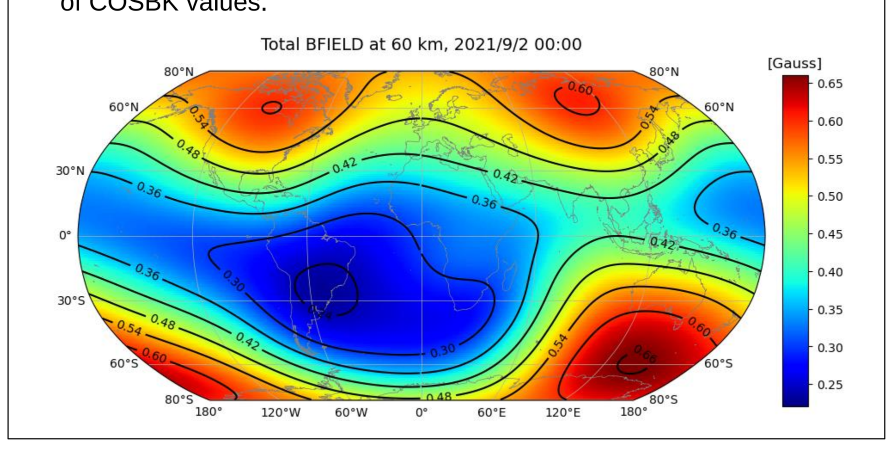

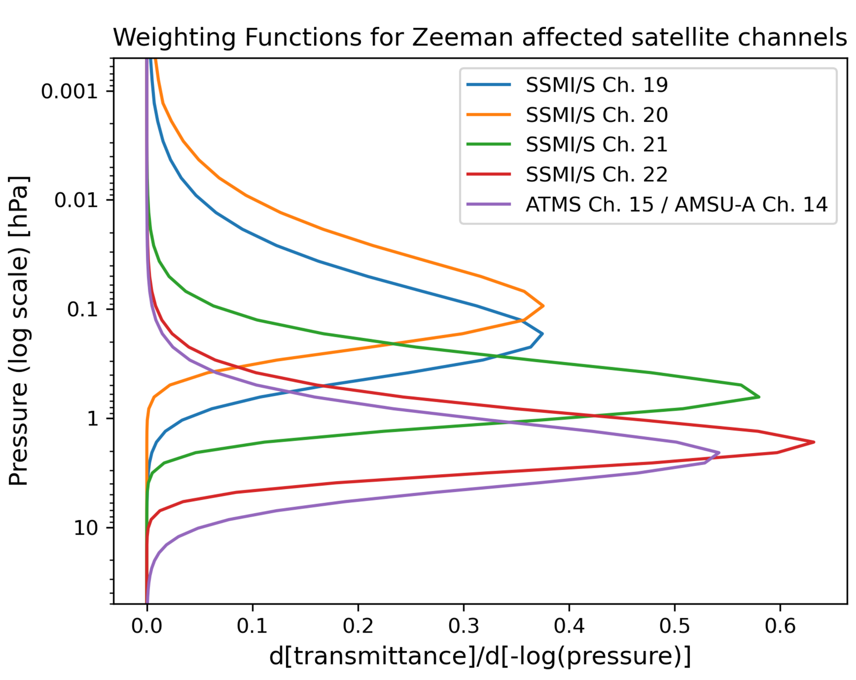

Channel SSMI/S	Central frequency [GHz]	Offset/s [± GHz]	Bandwidth [MHz]	Mean vertical peak [hPa / km]
19	63.283248	0.285271	1.3584	0.2 hPa / 55 km
20	60.792668	0.357892	1.3556	0.08 hPa / 60 km
21	60.792668	0.357892 ± 0.0020	1.2883	0.7 hPa / 45 km
22	60.792668	0.357892 ± 0.0055	2.6239	1.7 hPa / 40 km
ATMS/AMSU-A				
15/14	57.290344	0.3222 ± 0.0045	3.0	1.9 hPa / 40 km

Table 4. High peaking channel characteristics for SSMI/S and ATMS/AMSU-A

ATMS channel 15

The Advanced Technology Microwave Sounder (ATMS) is not strongly affected by the Zeeman effect in channel 15 (~0.2 K magnitude for most of the globe). Differences can reach 0.5 K in southern high latitudes. Satellite zenith angle has little effect.

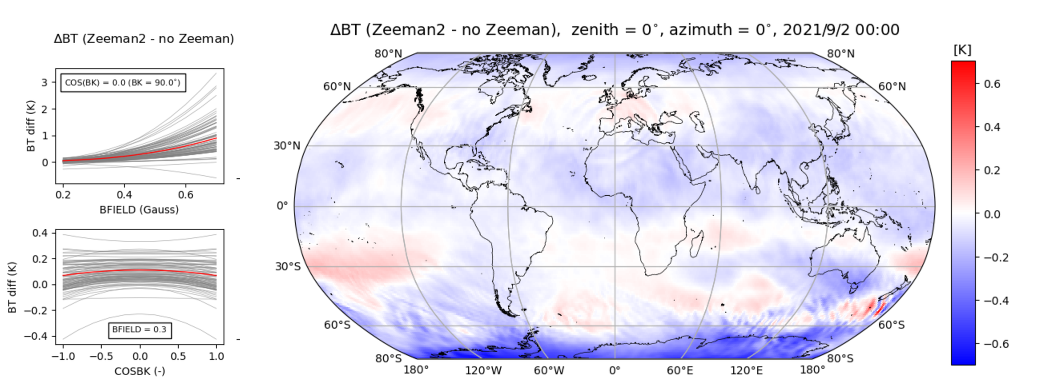

SSMI/S channels 19-22

Simulations of Zeeman affected TOA brightness temperatures (BT) in the high peaking channels of the Special Sensor Microwave Imager/Sounder (SSMI/S) can deviate strongly from non-Zeeman simulations. In equatorial regions Zeeman radiances can be up to 10 K lower in channel 20. Channel 22, however, shows only minor effects up to ~0.2 K. The general pattern of negative and positive differences is reversed between pairs of channels 19-20 and 21-22 because of the different predictors used (Table 3).

Interestingly, the largest differences in channel 20 (> 10 K) are at low magnetic field values of 0.3 Gauss.

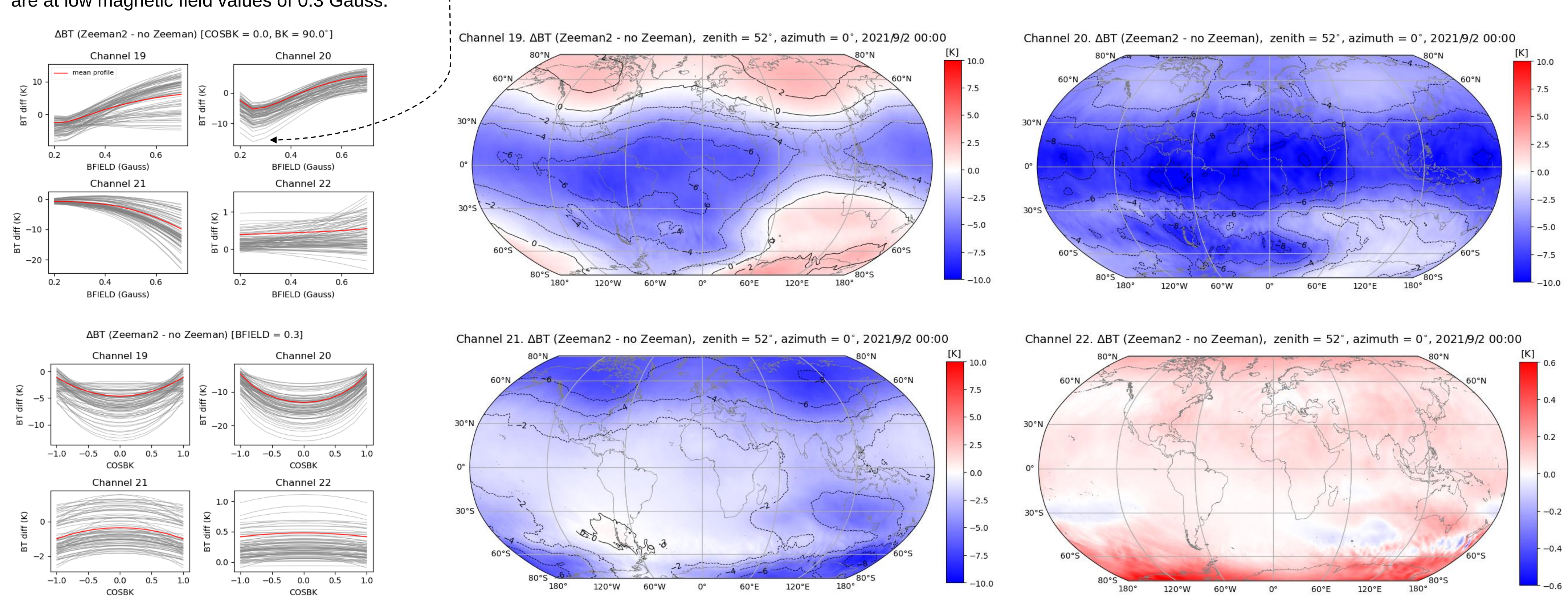

Validation statistics

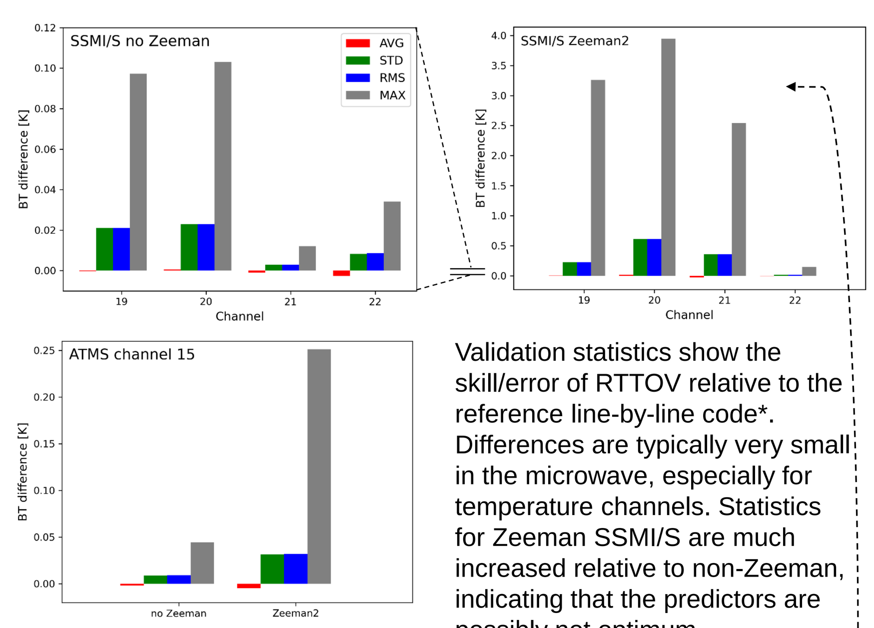

Validation statistics show the skill/error of RTTOV relative to the reference line-by-line code*. Differences are typically very small in the microwave, especially for temperature channels. Statistics for Zeeman SSMI/S are much increased relative to non-Zeeman, indicating that the predictors are possibly not optimum.

* https://nwp-saf.eumetsat.int/site/software/rttov/download/coefficients/comparison-with-lbl-simulations/

References
Alken, P., Thébault, E., Beggan, C.D. *et al.* "International Geomagnetic Reference Field: the thirteenth generation." *Earth Planets Space* 73, 49 (2021). https://doi.org/10.1186/s40623-020-01288-x
Hocking, J., et al. "A new gas absorption optical depth parameterisation for RTTOV version 13." Geoscientific Model Development 14.5 (2021): 2899-2915.
Larsson, R., Lankhaar, B., and Eriksson, P. "Updated Zeeman effect splitting coefficients for molecular oxygen in planetary applications." *Journal of Quantitative Spectroscopy and Radiative Transfer* 224 (2019): 431-438.
Liebe, H. J., Rosenkranz, PW., and Hufford, GA. "Atmospheric 60-GHz oxygen spectrum: New laboratory measurements and line parameters." *Journal of Quantitative Spectroscopy and Radiative Transfer* 48.5-6 (1992): 629-643.
Rosenkranz, P.W.: Line-by-line microwave radiative transfer (non-scattering), *Remote Sens. Code Library*, doi:10.21982/M81013, (2017)
Rosenkranz, PW., and Staelin, DH. "Polarized thermal microwave emission from oxygen in the mesosphere." *Radio Science* 23.05 (1988): 721-729.
Tretyakov, M. Yu, et al. "60-GHz oxygen band: precise broadening and central frequencies of fine-structure lines, absolute absorption profile at atmospheric pressure, and revision of mixing coefficients." *Journal of Molecular Spectroscopy* 231.1 (2005): 1-14.

Met Office FitzRoy Road, Exeter, Devon, EX1 3PB United Kingdom
Tel: +44 1392 885680 Fax: +44 1392 885681
Email: name.name@metoffice.gov.uk